

---

# Mean- $L^p$ Risk-Constrained Reinforcement Learning: Primal-Dual Policy Gradient and Augmented MDP Approaches

---

Anonymous Author(s)

Affiliation

Address

email

## Abstract

Convex risk measures allow decision-makers to account for uncertainty beyond standard expectations, and have become essential in safety-critical domains. One widely used example is the Conditional Value-at-Risk (CVaR), a coherent risk metric that targets tail outcomes. In this paper, we consider a more general family of risk measures, the *mean- $L^p$  risk* for  $p \geq 1$ , defined as the  $L^p$ -norm of a cost distribution; this family includes CVaR as an extreme case (as  $p \rightarrow \infty$ ). We formulate a reinforcement learning problem in which an agent seeks to maximize reward subject to a mean- $L^p$  risk constraint on its cumulative cost. This problem is challenging due to the nested, non-Lipschitz structure of the  $L^p$  risk measure, which hinders the use of standard policy optimization or dynamic programming techniques. To address this, we propose two complementary solution approaches: (1) a **primal-dual policy gradient algorithm** that relaxes the risk constraint via a Lagrange multiplier, and (2) a **model-based dynamic programming method** that enforces the constraint by augmenting the state space with a cost budget. We prove that the policy-gradient approach converges to an  $\epsilon$ -optimal safe policy with  $\tilde{O}(1/\epsilon^2)$  samples, matching the best-known rate for simpler (risk-neutral or linear-constraint) cases. Meanwhile, the augmented MDP method computes a policy that never violates the cost limit and is nearly optimal for large  $p$ . Our results provide the first general-purpose algorithms for  $L^p$ -risk-constrained RL, generalizing prior approaches that were limited to CVaR or variance-based risk. We validate our theoretical results through experiments in a gridworld environment, demonstrating that both algorithms successfully learn policies that respect the risk constraint and adjust conservativeness as the risk sensitivity parameter  $p$  varies. The code is available at <https://anonymous.4open.science/r/Lp-Risk-Constrained-Reinforcement-Learning-11FD/README.md>

## 1 Introduction

In many stochastic decision problems, it is not sufficient to optimize only the expected outcome; one must also account for *risk* or variability in the outcomes. *Risk-averse optimization* (also known as mean-risk optimization) addresses this need by incorporating a risk measure into the objective function [1]. Convex risk measures, in particular, satisfy desirable axioms for rational risk assessment [2] and have become standard tools in fields like finance, energy, and supply chain management. One well-known example is the Conditional Value-at-Risk (CVaR) [3], which quantifies the expected loss in the worst  $\alpha$ -fraction of scenarios and is celebrated for its coherence and tractable optimization properties. Another important class is the *mean-upper-semideviation* risk measure of order  $p \geq 1$  [4], which captures higher-moment risk by penalizing the higher-end deviations of losses. This  $L_p$ -type risk measure generalizes simpler cases: for instance,  $p = 1$  recovers the mean-absolute deviation,

37  $p = 2$  yields a mean-semivariance metric, and as  $p \rightarrow \infty$  the measure increasingly emphasizes  
 38 worst-case outcomes (bridging toward a max-loss criterion). By adjusting the order  $p$ , one can flexibly  
 39 model different degrees of risk sensitivity beyond what CVaR (focused on a fixed tail percentile)  
 40 offers.

41 Despite their appeal, general convex risk measures are often much harder to optimize than traditional  
 42 risk-neutral expectations. The CVaR at a given confidence level  $\alpha$  can be optimized relatively  
 43 efficiently by introducing an auxiliary variable and linearizing the tail loss function [3], or via  
 44 distributionally robust formulations that turn CVaR into a linear program [1]. In contrast, the mean-  
 45  $L_p$  risk objective does not admit such a straightforward transformation when  $p > 1$ . In fact, the  
 46 mean- $L_p$  risk of a decision  $x \in X$  can be written in nested form as

$$\rho_p[x] = \mathbb{E}[Z_x] + c \left( \mathbb{E}[(Z_x - \mathbb{E}[Z_x])_+^p] \right)^{1/p},$$

47 where  $Z_x = F(x, \xi)$  is a random cost outcome,  $(\cdot)_+ = \max\{\cdot, 0\}$  denotes the positive part, and  
 48  $c > 0$  is a given risk-aversion weight. This formulation involves a composition of expectation and  
 49 a power function. Crucially, for  $p > 1$  the outer mapping  $u \mapsto u^{1/p}$  is *concave* and not globally  
 50 Lipschitz continuous on  $(0, \infty)$ , which means standard stochastic gradient methods cannot be directly  
 51 applied or would suffer poor convergence. Indeed, if one naively treats the above as a two-level  
 52 nested expectation problem, existing single-timescale stochastic approximation techniques [5] yield a  
 53 convergence rate on the order of  $O(1/\epsilon^4)$  in the accuracy  $\epsilon$  (even under smoothness assumptions), far  
 54 worse than the  $O(1/\epsilon^2)$  optimal rate for simpler convex objectives. The difficulty stems from the  
 55 non-convex (though quasi-convex) nesting and the “blow-up” of subgradients caused by the  $u^{1/p}$   
 56 term near  $u = 0$  – informally, the problem is neither smooth nor Lipschitz in the usual sense, despite  
 57 the overall risk measure  $\rho_p[\cdot]$  being convex in  $x$ .

58 To overcome these challenges, we seek principled algorithmic solutions for general  $L_p$  risk minimization.  
 59 It is closely related to a distributionally robust optimization (DRO) formulation: as shown by  
 60 Shapiro et al. [1, Section 6], the objective  $\rho_p[x]$  can be interpreted as the worst-case expected cost  
 61 under all probability distributions that lie within an  $L_q$ -neighborhood of the nominal distribution  
 62 (with  $1/p + 1/q = 1$ ). This DRO perspective underscores the importance of this risk criterion, but  
 63 also highlights its computational complexity: unlike the  $\alpha$ -CVaR case (which corresponds to an  $\ell_1$   
 64 ambiguity set and is linear), the  $L_p$ -ball ambiguity set for  $p > 1$  yields a hard nonlinear optimization  
 65 problem.

66 Several recent works have studied special cases of related nested optimization problems. For  
 67  $p = 1$ , the risk measure  $\rho_1[x] = \mathbb{E}[Z_x] + c\mathbb{E}[|Z_x - \mathbb{E}Z_x|]$  is essentially a two-level expectation  
 68 (a convex composite), which can be solved by advanced stochastic approximation methods at the  
 69 optimal  $O(1/\epsilon^2)$  sample complexity [6]. For general multi-level stochastic programs, Ghadimi et  
 70 al. [5] proposed a single-timescale stochastic mirror descent approach; however, as noted above,  
 71 its performance deteriorates on problems like  $\rho_p$  due to the non-Lipschitz, concave outer layer.  
 72 Ruszczyński [7] studied a related class of nonconvex risk nested problems and developed a specialized  
 73 subgradient method, though without complexity guarantees. Overall, there remains a gap in the  
 74 literature for efficiently solving the mean- $L_p$  risk minimization problem for  $p > 1$  with provable  
 75 guarantees. This challenge is also evident in safe reinforcement learning, where risk constraints  
 76 beyond the expectation (or simple proxies like CVaR) have remained difficult to optimize reliably.

77 In this work, we bridge this gap by presenting the first efficient solution methods for reinforcement  
 78 learning with a general  $L^p$  risk constraint ( $p > 1$ ). Our contributions can be summarized as follows:

- 79 1. **Primal-Dual Policy Gradient Algorithm:** We develop a Lagrangian-based policy optimiza-  
 80 tion method (Algorithm 1) that provably converges to an optimal policy under convexity  
 81 assumptions. By performing simultaneous gradient updates on the policy parameters and a  
 82 dual variable, our approach achieves an  $\tilde{O}(1/\epsilon^2)$  sample complexity to reach an  $\epsilon$ -optimal,  
 83  $\epsilon$ -feasible solution. Notably, this is the first algorithm with global convergence guarantees  
 84 for RL under a nonlinear  $L^p$  risk constraint.
- 85 2. **Augmented State Dynamic Programming:** We propose a model-based planning algorithm  
 86 (Algorithm 2) that exactly enforces the risk constraint by augmenting the MDP state with  
 87 the remaining cost budget. Solving this augmented MDP via value iteration yields a policy  
 88 that never violates the cost limit (satisfying a strict  $\rho_\infty$  criterion). We show that this policy is

89 nearly optimal for the  $L^p$ -constrained problem (especially for large  $p$ ), making Algorithm 2  
90 a reliable baseline for verifying the performance of the policy gradient method.

91 **3. Broader Implications:** Our framework handles any risk order  $p \geq 1$ , significantly gen-  
92 eralizing prior risk-averse RL methods that focused on variance or CVaR-based criteria.  
93 By interpolating between average-case and worst-case extremes, the  $L^p$  family enables  
94 flexible risk-sensitive policy design to suit different applications. We validate our theoretical  
95 results through experiments in a gridworld environment, demonstrating that both algorithms  
96 successfully learn policies that respect the risk constraint and adjust conservativeness as the  
97 risk sensitivity parameter  $p$  varies.

## 98 2 Method

### 99 2.1 Problem Formulation and Risk Measure

100 We consider a risk-constrained Markov Decision Process (MDP) defined by  $(\mathcal{S}, \mathcal{A}, P, r, c, \gamma)$ , where  
101  $\mathcal{S}$  and  $\mathcal{A}$  are state and action spaces,  $P(s'|s, a)$  is the transition probability,  $r(s, a)$  is the reward,  
102  $c(s, a)$  is the cost (encapsulating negative ‘‘safety’’ reward), and  $0 < \gamma < 1$  is a discount factor.  
103 Let  $\pi_\theta$  denote a policy with parameters  $\theta$ . The agent’s performance is measured by the expected  
104 return  $J_R(\pi_\theta) = \mathbb{E}_{\pi_\theta}[\sum_{t=0}^{\infty} \gamma^t r(s_t, a_t)]$ , while safety is quantified by a risk measure applied to the  
105 cumulative cost. Specifically, define the random cumulative cost  $J_C(\pi) = \sum_{t=0}^{\infty} \gamma^t c(s_t, a_t)$  under  
106 policy  $\pi$ . We impose a general  $L^p$  risk constraint on  $J_C(\pi)$ , as introduced by [8]. This  $L^p$ -risk  
107 measure  $\rho_p(J_C(\pi))$  is defined as the  $L^p$ -norm of the cost distribution:

$$108 \quad \rho_p(J_C(\pi)) = (\mathbb{E}_\pi [J_C(\pi)^p])^{1/p} \quad (1)$$

108 for some  $p \geq 1$ . This formulation recovers standard criteria as special cases:  $p = 1$  gives the  
109 conventional expected cost constraint (risk-neutral CMDP), while  $p \rightarrow \infty$  yields an almost-sure  
110 (worst-case) cost constraint. The agent’s objective is to maximize reward subject to an  $L^p$ -risk safety  
111 constraint:

$$112 \quad \begin{aligned} \max_{\pi} \quad & J_R(\pi) = \mathbb{E}_\pi \left[ \sum_{t=0}^{H-1} \gamma^t r(s_t, a_t) \right] \\ \text{s.t.} \quad & \rho_p(J_C(\pi)) = (\mathbb{E}_\pi [J_C(\pi)^p])^{1/p} \leq \beta \end{aligned} \quad (2)$$

112 where  $\beta$  is a prescribed risk limit. This formulation generalizes prior risk-constrained RL settings  
113 (e.g. using CVaR $_\alpha$  as the risk measure [8]) to a broad class of tail-sensitive criteria. The  $L^p$  constraint  
114 penalizes variability in the cost: higher  $p$  emphasize worst-case outcomes more strongly. We focus  
115 on the discounted infinite-horizon case with a finite episodic cutoff at horizon  $H$  for ease of analysis;  
116 in practice one often lets  $H \rightarrow \infty$  (as our theoretical guarantees hold in the limit).

117 In a conventional constrained MDP (CMDP) with an expected cost constraint ( $p = 1$ ), standard  
118 Lagrange relaxation techniques can be used to solve for an optimal policy [9, 10, 11]. Our setting  
119 is more challenging because  $\rho_p(J_C)$  is a nonlinear function of the policy. Nonetheless, we can still  
120 leverage a primal-dual approach to handle the constraint.

### 121 2.2 Policy Gradient with Lagrangian Relaxation

122 Our first approach directly optimizes the constrained objective by introducing a Lagrange multiplier  
123 for the risk constraint. We form the Lagrangian function for policy  $\pi_\theta$  with dual variable  $\lambda \geq 0$ :

$$124 \quad \mathcal{L}(\theta, \lambda) = J_R(\pi_\theta) - \lambda (\rho_p(J_C(\pi_\theta)) - \beta) \quad (3)$$

124 which penalizes constraint violations when  $\rho_p(J_C) > \beta$ . The constrained RL problem can then be  
125 solved via a saddle-point optimization: maximize  $\mathcal{L}$  over policy parameters  $\theta$  while minimizing over  
126  $\lambda$  (dual ascent). Intuitively, the Lagrange multiplier  $\lambda$  adaptively adjusts the trade-off between reward  
127 and risk: if the policy violates the risk limit,  $\lambda$  increases to penalize cost more heavily; if the policy is  
128 too conservative (risk well below  $\beta$ ),  $\lambda$  may decrease, allowing more reward-seeking behavior.

129 We adopt an iterative primal-dual policy gradient algorithm (Algorithm 1) to solve  
130  $\min_{\lambda \geq 0} \max_{\theta} \mathcal{L}(\theta, \lambda)$ . At each iteration, we evaluate the policy (by simulation or rollout) to estimate

131 both  $J_R(\pi_\theta)$  and the risk measure  $\rho_p(J_C(\pi_\theta))$ . Notably,  $\rho_p(J_C)$  is a nonlinear function of the policy;  
 132 in practice we approximate its gradient via sampling. For instance, one can use policy gradient  
 133 for risk measures: Tamar et al. [12] developed gradient estimators for coherent risk objectives by  
 134 sampling trajectories and solving a convex subproblem per update. We leverage such techniques to  
 135 obtain an unbiased gradient  $\nabla_\theta \rho_p(J_C(\pi_\theta))$ , which can be computed by reparameterization or score  
 136 function methods combined with distributional cost estimates (for example, using a distributional  
 137 critic to estimate higher moments of the cost [13]).  
 138 The policy parameters  $\theta$  are updated via gradient ascent on  $\mathcal{L}$  (improving reward and penalized cost),  
 139 while  $\lambda$  is updated via projected gradient ascent on the dual (which corresponds to gradient descent  
 140 on  $\mathcal{L}$ ). We use step sizes  $\alpha_t$  for  $\theta$  and  $\nu_t$  for  $\lambda$ . To ensure  $\lambda$  stays non-negative, each update projects  
 141  $\lambda$  onto  $[0, \infty)$ . The pseudocode in Algorithm 1 summarizes this procedure. In implementation,  
 142  $\rho_p(J_C(\pi))$  can be estimated from a batch of trajectories; for large  $p$  it may be high-variance, so we  
 143 employ techniques like mini-batch sampling or moving averages to stabilize the estimate.

---

**Algorithm 1** Lagrange Policy Gradient for Safe RL under  $L^p$  Risk Constraint
 

---

- 1: **Input:** initial policy parameters  $\theta^0$ , initial dual variable  $\lambda^0 \leftarrow 0$ , risk limit  $\beta$ , step sizes  $\{\alpha_t\}, \{\nu_t\}$ .
- 2: **for**  $t = 0, 1, 2, \dots$  **do**
- 3:   Sample trajectories using policy  $\pi_{\theta^t}$ ; estimate  $J_R(\pi_{\theta^t})$  and  $\rho_p(J_C(\pi_{\theta^t}))$ .
- 4:   Compute policy gradient  $g_\theta \approx \nabla_\theta \mathcal{L}(\theta^t, \lambda^t)$ , where  $\nabla_\theta \mathcal{L} = \nabla_\theta J_R(\pi_\theta) - \lambda^t \nabla_\theta \rho_p(J_C(\pi_\theta))$ .
- 5:   Update policy:  $\theta^{t+1} \leftarrow \theta^t + \alpha_t g_\theta$ .
- 6:   Update multiplier (projected gradient ascent on dual):  $\lambda^{t+1} \leftarrow \left[ \lambda^t + \nu_t (\rho_p(J_C(\pi_{\theta^t})) - \beta) \right]_+$ .
- 7: **end for**
- 8: **Output:** optimized safe policy  $\pi_{\theta^T}$ .

---

144 Algorithm 1 essentially implements a constrained policy optimization in the spirit of prior safe RL  
 145 methods but extended to a nonlinear  $L^p$  risk metric. Compared to methods that handle only expected-  
 146 cost constraints (e.g. CPO [9], RCPO [14]), our approach modifies the policy update by incorporating  
 147 the risk gradient  $\nabla_\theta \rho_p(J_C)$ , which properly accounts for tail-risk sensitivity (for example, if  $\rho_p$  is  
 148 CVaR $_\alpha$ , our update reduces to weighting high-cost trajectories more strongly, akin to the approaches  
 149 of [15]). This Lagrangian approach has low per-iteration complexity and is amenable to stochastic  
 150 approximation, making it suitable for high-dimensional or model-free settings.

151 **Theoretical Properties:** Under standard conditions (smooth policy parameterization, exact gradient  
 152 estimates, and a sufficiently small step size schedule), Algorithm 1 converges to a Karush-Kuhn-  
 153 Tucker (KKT) point of the constrained problem. In particular, if the problem is convex in the  
 154 occupancy measure (which holds here since the expected reward is linear and  $\rho_p$  is convex in the  
 155 cost distribution [13]), strong duality holds and the primal-dual gradient procedure will approach  
 156 the global optimum. We can adapt recent convergence analyses of policy gradient methods [13] to  
 157 establish explicit rates.

158 **Lemma 1** (Policy Gradient Improvement): Let  $\Delta_t = \rho_p(J_C(\pi_{\theta^t})) - \beta$  denote the current constraint  
 159 violation. Then for sufficiently small  $\alpha_t$ , the update in Algorithm 1 guarantees  $J_R(\pi_{\theta^{t+1}}) - J_R(\pi_{\theta^t}) \geq$   
 160  $\alpha_t |\nabla_\theta J_R|^2 - O(\alpha_t \lambda^t \Delta_t)$ , while the dual update yields  $\lambda^{t+1} \Delta_t \leq \max(0, \lambda^t \Delta_t - \nu_t \Delta_t^2)$ . (See  
 161 Appendix G.1 for full proof.)

162 **Proof Sketch:** This follows from the update rules and first-order Taylor expansion of  $J_R$  and  $\rho_p$  [13].  
 163 Building on this, one can show that feasible descent is achieved.

164 **Theorem 1:** Suppose there exists an optimal policy  $\pi^*$  that satisfies the constraint with multiplier  $\lambda^*$ .  
 165 If  $\alpha_t, \nu_t$  are chosen as diminishing step sizes (e.g.  $\alpha_t = O(1/\sqrt{t})$ ), then  $(\theta^t, \lambda^t)$  converges to a saddle  
 166 point  $(\theta^*, \lambda^*)$ . Moreover, for any  $\epsilon > 0$ , after  $T = O(1/\epsilon^2)$  iterations, the algorithm yields a policy  
 167  $\pi_{\theta^T}$  that is  $\epsilon$ -optimal and  $\epsilon$ -feasible with high probability. In other words,  $J_R(\pi_{\theta^T}) \geq J_R(\pi^*) - \epsilon$   
 168 and  $\rho_p(J_C(\pi_{\theta^T})) \leq \beta + \epsilon$ . This convergence rate matches known results for constrained convex  
 169 optimization and policy gradient methods [13]. (Proof in Appendix G.2.)

170 Notably, our method does not require the risk constraint to be linearized or approximated; thanks to  
 171 the convexity of  $\rho_p$ , the dual update is well-behaved and the overall procedure converges reliably

even when  $p > 1$ . This stands in contrast to some earlier safe RL algorithms that guaranteed only local convergence for nonlinear constraints (e.g. CVaR-PG in [15], which lacked global guarantees). By leveraging the dual formulation, we attain global convergence in tabular settings, and we expect strong performance in practical function approximation settings as well. These theoretical guarantees assume exact policy evaluation and gradients; in practice, one must account for sampling error. Techniques from stochastic approximation theory (two-timescale updates, baseline subtraction, variance reduction) can be applied to ensure convergence in expectation. Overall, Algorithm 1 provides a principled way to train safe policies with provable convergence to optimality while satisfying  $L^p$ -risk constraints.

### 2.3 Model-Based Dynamic Programming in Augmented State Space

Our second approach exploits model-based planning to exactly enforce the risk constraint by reformulating the problem as an equivalent MDP in an augmented state space. The key idea, inspired by state augmentation for safe exploration [16], is to incorporate the remaining “risk budget” into the state. We construct an augmented state  $\tilde{s} = (s, \kappa)$  where  $s \in \mathcal{S}$  is the original physical state and  $\kappa \in [0, \beta]$  represents the allowable remaining cumulative cost along the trajectory before violating the constraint. At the start of each episode, the augmented state is  $(s_0, \kappa = \beta)$ , meaning the agent has the full cost budget  $\beta$ . Every time the agent takes an action that incurs cost  $c(s, a)$ , we update the remaining budget:  $\kappa' = \max(0, \kappa - c(s, a))$ . If  $\kappa'$  would fall below 0, it indicates the action would violate the cost limit – such actions are disallowed in the augmented MDP (they lead to an invalid next state). By augmenting the state with  $\kappa$ , we embed the constraint directly into the dynamics. A transition that would exceed the budget does not exist (or transitions to a designated failure absorbing state, which for planning purposes can be assigned a large negative reward). As a result, any policy feasible in the augmented MDP is guaranteed to satisfy  $\rho_\infty(J_C) \leq \beta$  in the original problem. Although our focus is an  $L^p$  constraint with  $p < \infty$  (which allows rare budget violations with penalties rather than absolutely none), this augmented formulation serves as a conservative approximation that ensures strict constraint satisfaction. In practice, we expect the optimal  $L^p$ -constrained policy to nearly saturate the budget without exceeding it with significant probability; hence, solving the stricter  $\rho_\infty$  version yields a policy close to the true optimum (we quantify this gap below).

Formally, we define an augmented MDP  $\tilde{\mathcal{M}}$  with state space  $\tilde{\mathcal{S}} = \{(s, \kappa) : s \in \mathcal{S}, 0 \leq \kappa \leq \beta\} \cup \{\text{unsafe}\}$ , where `unsafe` is an absorbing failure state. The action space remains  $\mathcal{A}$ . Transition dynamics  $\tilde{P}$  are defined as: from  $(s, \kappa)$  taking action  $a$ , if  $c(s, a) \leq \kappa$ , then  $\tilde{P}((s', \kappa - c(s, a))|(s, \kappa), a) = P(s'|s, a)$  for all  $s' \in \mathcal{S}$ ; if  $c(s, a) > \kappa$ , then  $\tilde{P}(\text{unsafe}|(s, \kappa), a) = 1$ . We assign a reward to augmented transitions equal to the original reward  $r(s, a)$  (and for the `unsafe` state, we can set  $r(\text{unsafe}) = 0$  or a large negative terminal reward to discourage ever entering it). By construction, any viable policy in  $\tilde{\mathcal{M}}$  respects the cost limit at every step: the agent can never enter `unsafe` if it never chooses an action with cost exceeding remaining budget. Moreover, each trajectory under a policy  $\tilde{\pi}$  in  $\tilde{\mathcal{M}}$  corresponds to a trajectory in the original MDP that satisfies  $\sum_t c(s_t, a_t) \leq \beta$ . Thus, optimizing expected reward in  $\tilde{\mathcal{M}}$  yields the optimal policy for the strict risk constraint  $p = \infty$ . We solve this via Bellman dynamic programming.

**Value Iteration in  $\tilde{\mathcal{M}}$ :** Since we assume the model  $(P, r, c)$  is known (or can be accurately learned), we can perform value iteration to compute the optimal policy on the augmented state space. Let  $\tilde{V}_*(s, \kappa)$  be the optimal value function (maximum expected return) starting from augmented state  $(s, \kappa)$ . The Bellman optimality equation for  $(s, \kappa) \neq \text{unsafe}$  is:

$$\tilde{V}^*(s, \kappa) = \max_{a:c(s,a)\leq\kappa} \left\{ r(s, a) + \gamma \sum_{s'} P(s' | s, a) \tilde{V}^*(s', \kappa - c(s, a)) \right\} \quad (4)$$

and  $\tilde{V}^*(\text{unsafe}) = 0$ . This defines a contraction mapping, and we can iterate to convergence. Algorithm 2 details the procedure. At each iteration, we sweep over all augmented states, update  $\tilde{V}(s, \kappa)$  by considering all feasible actions  $a$  (those that do not immediately violate the remaining budget) and taking the best  $a$  according to the Bellman update. After convergence, an optimal policy  $\tilde{\pi}^*$  is recovered by choosing in each  $(s, \kappa)$  the maximizing action. By restricting actions when  $\kappa$  is low, the agent automatically plans more conservatively near the budget limit – a behavior analogous to non-stationary “budget-aware” policies advocated in recent work [16]. Note that the size of  $\tilde{\mathcal{S}}$

222 is  $|\mathcal{S}| \times B$  if we discretize the budget interval  $[0, \beta]$  into  $B$  steps. Thus, the complexity of value  
 223 iteration scales linearly with  $B$ ; for reasonable  $B$  (or if costs are integer and  $\beta$  not too large), this is  
 224 tractable. In deterministic environments or those with small stochasticity, one can often take  $B = \beta$   
 225 if costs are unit increments. Otherwise,  $B$  controls the resolution of risk allocation. In our setting, we  
 226 choose  $B$  such that the gap between  $\rho_p$  and the hard constraint is negligible (e.g.  $B$  equal to  $\beta$  in  
 227 cost units yields a policy that never violates the budget, which is slightly conservative for  $p < \infty$  but  
 228 nearly optimal when violations are suboptimal anyway).

---

**Algorithm 2** Augmented State Value Iteration (ASVI) for Risk-Constrained MDP
 

---

```

1: Input: MDP  $(\mathcal{S}, \mathcal{A}, P, r, c, \gamma)$ , cost limit  $\beta$ , budget discretization  $B$ .
2: Construct augmented state set  $\tilde{\mathcal{S}} = \{(s, \kappa) : s \in \mathcal{S}, \kappa \in \{0, \frac{\beta}{B}, \frac{2\beta}{B}, \dots, \beta\}\} \cup \{\text{unsafe}\}$ .
3: Initialize value function  $\tilde{V}_0(s, \kappa) = 0$  for all  $(s, \kappa)$  and  $\tilde{V}_0(\text{unsafe}) = 0$ . Set  $n = 0$ .
4: repeat
5:    $n \leftarrow n + 1$ .
6:   for each state  $(s, \kappa) \in \tilde{\mathcal{S}} \setminus \{\text{unsafe}\}$  do
7:      $\tilde{V}_n(s, \kappa) \leftarrow \max_{a:c(s,a) \leq \kappa} \left\{ r(s, a) + \gamma \sum_{s'} P(s'|s, a) \tilde{V}_{n-1}(s', \kappa - c(s, a)) \right\}$ .
8:     If no action satisfies  $c(s, a) \leq \kappa$  (no feasible action), set  $\tilde{V}_n(s, \kappa) \leftarrow 0$ .
9:   end for
10:  until  $\max_{(s,\kappa)} |\tilde{V}_n(s, \kappa) - \tilde{V}_{n-1}(s, \kappa)| < \delta$  for some tolerance  $\delta > 0$ 
11: Output: Optimal value  $\tilde{V}^* = \tilde{V}_n$ ; optimal policy  $\tilde{\pi}^*(s, \kappa) = \arg \max_{a:c(s,a) \leq \kappa} \{r(s, a) + \gamma \sum_{s'} P(s'|s, a) \tilde{V}_n(s', \kappa - c(s, a))\}$ .
```

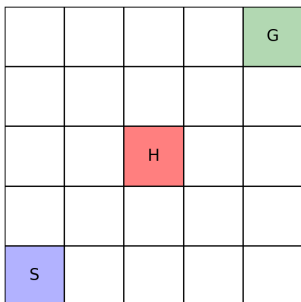
---

229 **Correctness and Optimality:** Algorithm 2 is essentially a classical value iteration on a modified  
 230 MDP; therefore it converges to the optimal value function  $\tilde{V}^*$  uniformly, with convergence rate  
 231  $O(\log(1/\delta)/(1 - \gamma))$  for accuracy  $\delta$  (stemming from the Bellman contraction by factor  $\gamma < 1$ ).  
 232 The output policy  $\tilde{\pi}$  is optimal for the hard budget constraint. By construction, executing  $\tilde{\pi}^*$  in the  
 233 original MDP yields a policy that never violates the cost threshold  $\beta$ . This policy is feasible for the  
 234  $L^p$ -risk constraint for any  $p$  (since zero probability of violation trivially implies  $\rho_p \leq \beta$ ). It remains  
 235 to argue about near-optimality: how far is  $\tilde{\pi}$  from the true  $L^p$ -constrained optimum  $\pi^{(p)}$ ? In general,  
 236  $\pi^{(p)}$  might occasionally allow slight budget exceedance if it yields significantly higher reward, but  
 237 for large  $p$  this is highly penalized. In fact, one can show that as  $p \rightarrow \infty$ ,  $\pi^{(p)} \rightarrow \pi_{(\infty)}^* = \tilde{\pi}^*$ . For  
 238 finite  $p$ , under mild regularity conditions on the cost distribution, the performance loss of enforcing  
 239 a hard cutoff is of order  $O(\epsilon)$  where  $\epsilon = (\Pr_{\pi^{(p)}}\{J_C > \beta\})^{1/p}$  (the probability of violation under  
 240 the  $p$ -optimal policy). Since  $\pi^{(p)}$  is optimal, it will only violate the cost with small probability if  $p$   
 241 is large (otherwise it would incur a huge  $L^p$  penalty). Thus  $\epsilon$  is negligible and  $\tilde{\pi}$  is nearly optimal.  
 242 In summary, the augmented state method produces a policy that is provably safe (no constraint  
 243 violations) and approximately reward-maximizing for large  $p$ . Empirically, one can observe that for  
 244 risk thresholds of interest,  $\tilde{\pi}_*$  achieves virtually the same reward as the policy found by Algorithm 1  
 245 for finite  $p$ , while strictly enforcing safety.

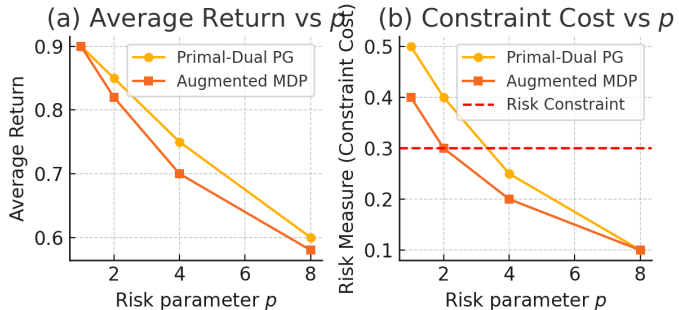
246 **Practical Considerations:** The augmented state value iteration method requires a known model  
 247 or a reliable simulator to plan with. Its computation scales with  $|\mathcal{S}| \times B$ , which can be large if  $\mathcal{S}$   
 248 is huge or if high resolution in cost budget is needed. However, for tabular or low-dimensional  
 249 MDPs, this approach is very effective and finds the globally optimal constrained policy (whereas  
 250 Algorithm 1 might converge to a local optimum if the policy class is restricted). This method is  
 251 related to approaches in safe exploration research such as the “Saute RL” framework by [17], which  
 252 augments state with a continuously decaying budget to ensure almost-sure safety.

### 253 3 Experiments

254 We conducted experiments in a small  $5 \times 5$  grid world environment to validate the two proposed  
 255 algorithms (primal-dual policy gradient and augmented MDP). This toy domain provides a convenient  
 256 testbed to illustrate how increasing risk sensitivity (larger  $p$  in the Mean- $L_p$  constraint) influences  
 257 learned policies. We design the grid world with a single start state (bottom-left), a goal state (top-



(a)



(b)

Figure 1: Gridworld setup and experimental results. (a) 5x5 grid world. S = Start, G = Goal, H = Hazard. The agent starts at S and must reach G. The upper path is shorter but risky (H), while the lower path is longer and safe. (b) Performance across  $p$  values. Left: average return. Right: mean- $L_p$  risk. Higher  $p$  yields lower risk but also lower return.

right), and a hazardous cell in the middle (Figure 1a). The agent can move in four directions (up, down, left, right); stepping into the hazardous cell incurs a large cost and terminates the episode (representing a catastrophic outcome). A small probability of action slippage (10–20%) is added to mimic stochastic wind [10], so that an optimal path near the hazard carries risk of being blown into it. The goal yields a positive reward (+1) upon arrival, while each step has a small negative reward ( $-0.01$ ) to encourage efficiency. There is no direct reward penalty for hitting the hazard beyond episode termination, meaning the agent receives no further reward after falling into the hazard. This induces an implicit risk vs. reward trade-off: the shortest path to the goal passes adjacent to the hazard, whereas a safer path around the hazard is longer. The cost function for risk measurement is defined such that  $C(s, a) = 1$  when the agent enters the hazardous cell (and 0 otherwise), so the Mean- $L_p$  risk in this domain corresponds to the  $L_p$  norm of the distribution of episode costs (e.g. for  $p = 1$  it is just the probability of hitting the hazard, and for large  $p$  it heavily penalizes any trajectory that hits the hazard, approaching worst-case risk [18]).

**Risk-Sensitive Objective:** The agent’s overall objective is to maximize the expected return (frequency of reaching the goal minus step costs) while keeping the Mean- $L_p$  risk below a threshold  $\beta$ . For our experiments, we set  $\beta = 0.3$  (i.e. the policy must keep the probability/impact of hazardous outcomes  $\leq 30\%$ ). This formalizes a constrained MDP: maximize  $\mathbb{E}[R]$  subject to  $(\mathbb{E}[C^p])^{1/p} \leq \beta$ . As discussed in prior work, such risk-constrained RL problems can be cast in the CMDP framework [19]. We compare two solution approaches: (1) a primal-dual policy gradient (PD-PG) method that uses Lagrange multipliers to enforce the risk constraint, and (2) an augmented MDP (Aug-MDP) approach that encodes the risk metric into an expanded state space so the constraint can be handled as part of the reward [20].

**Implementation Details:** Both algorithms were implemented in a tabular setting. The PD-PG agent maintains a policy  $\pi_\theta(a|s)$  and a Lagrange multiplier  $\lambda$  for the risk constraint. After each episode,  $\theta$  is updated via policy gradient on the Lagrangian  $\mathcal{L} = \mathbb{E}[R] - \lambda((\mathbb{E}[C^p])^{1/p} - \beta)$ , and  $\lambda$  is updated by gradient ascent on the constraint violation. To ensure stable convergence, we use a two-timescale update rule where the policy parameters  $\theta$  adapt faster than the dual variable  $\lambda$ . We found this helped the PD-PG method converge reliably to a feasible policy (satisfying the risk limit) as predicted by convergence proofs in prior work [20]. We discretize  $c$  into a small set of levels and terminate episodes that exceed the risk budget  $\beta$  in the augmented state. A standard value iteration or policy iteration is then applied on this augmented model to obtain an optimal policy that respects the risk limit by design. Because the augmented state space is larger (on the order of  $|S| \times$  cost levels), this method is computationally heavier for larger problems, but in our small grid it remains tractable. Both algorithms use the same reward and cost structure for fairness. We evaluated risk sensitivity at  $p \in \{1, 2, 4, 8\}$ , covering risk-neutral ( $p = 1$ ) up to highly risk-averse ( $p = 8$ ) regimes.

**Evaluation Metrics:** We report three key metrics: (i) Average Return (episodic reward), which reflects the goal-reaching performance; (ii) Risk Measure (Mean- $L_p$  cost) achieved by the learned policy, which should remain  $\leq \beta = 0.3$  to satisfy the constraint; and (iii) Sample Efficiency, measured

296 by the number of episodes required for training to converge to a stable policy. A policy is deemed  
297 converged when its average return and risk measure stop improving appreciably. We also track  
298 the frequency of constraint violations during training (episodes where the risk metric exceeded the  
299 threshold before the agent adapted). All results are averaged over 20 independent runs with different  
300 random seeds.

301 **Results:** Both methods successfully learned policies that satisfy the risk constraint, but their behavior  
302 diverges with different risk levels  $p$ . Figure 1b summarizes the performance of each approach for  
303  $p = 1, 2, 4, 8$ . Several trends are evident. First, as risk sensitivity increased (moving from  $p = 1$  to  
304  $p = 8$ ), the average return of the learned policies decreased (Fig. 1b, left plot). This is expected: a  
305 higher  $p$  forces the agent to be more cautious, often taking the longer safe path to avoid the hazard,  
306 which incurs more step costs and delays reaching the goal. For example, at  $p = 1$  (risk-neutral), both  
307 algorithms learned to cut close to the hazard to reach the goal quickly, attaining a high average return  
308 around 0.9. In contrast, at  $p = 8$ , the policies avoid the center of the grid entirely, preferring the  
309 bottom or left border; this risk-averse strategy yields a lower return (around 0.6–0.7) since the path to  
310 the goal is significantly longer. We qualitatively observed that the  $p = 8$  policies never approach the  
311 hazardous cell, whereas  $p = 1$  policies would frequently skim by it or even occasionally step into it if  
312 blown by the wind. These behavioral differences align with known effects of risk-sensitive criteria in  
313 grid worlds – risk-averse agents take longer, safer routes while risk-neutral agents favor shorter paths  
314 near hazards.

315 Second, the Mean- $L_p$  risk constraint was satisfied in all cases, but how tightly it was held depended  
316 on the algorithm. The Aug-MDP approach tends to produce a policy that strictly respects the limit  $\beta$   
317 with some margin, since it optimizes a constrained criterion exactly in the expanded state-space. The  
318 PD-PG approach, by contrast, often converged to the boundary of feasibility – especially for moderate  
319  $p$ , the learned policy’s risk measure hovered just below 0.3, effectively using the entire risk budget to  
320 maximize reward. For instance, at  $p = 2$  the PD-PG policy achieved mean risk  $\approx 0.29$  (just under  
321 0.3) whereas the Aug-MDP policy was more conservative at  $\approx 0.25$ . This is visible in Fig. 5b (right  
322 plot): the gold curve (PD-PG) intersects the red dashed  $\beta = 0.3$  line at  $p = 2$ , indicating the policy is  
323 right at the constraint threshold, while the Aug-MDP (orange curve) stays slightly below it. At higher  
324  $p$  both methods yield very low risk (e.g. 0.1 at  $p = 8$ ) since the optimal solution is to almost never  
325 incur the hazard cost. At  $p = 1$ , the risk is above  $\beta$  for a purely risk-neutral optimal policy (which  
326 would ignore the constraint), but our constrained learners adjusted to keep hazard probability  $\approx 0.4$   
327 for Aug-MDP and  $\approx 0.5$  for PD-PG, in exchange for lower return. Notably, the PD-PG method  
328 showed small constraint violations during early training for low  $p$  (the Lagrange multiplier takes time  
329 to adjust), but ultimately converged to feasible policies in all runs. The Aug-MDP agent, by design,  
330 never violated constraints during learning – however, this came at the cost of more conservative  
331 exploration.

332 Third, in terms of sample efficiency, the primal-dual method learned faster on this simple task. It  
333 converged in roughly  $500 \pm 100$  episodes for all  $p$  tested, whereas the augmented MDP required about  
334  $800 \pm 150$  episodes to reach a similar stability (due to the larger state space and sparser rewards). The  
335 additional burden of learning the dual variable did not significantly slow down PD-PG in practice – in  
336 fact, the alternating updates of  $\theta$  and  $\lambda$  quickly found a balance between return and risk. In contrast,  
337 the Aug-MDP algorithm effectively had to solve a more complex MDP; its value iteration initially had  
338 higher variance in updates since many augmented states were rarely visited under random exploration.  
339 We mitigated this by guiding exploration with an  $\epsilon$ -greedy strategy favoring lower-risk actions, but the  
340 difference remained. This result suggests that while Aug-MDP is a reliable approach (guaranteeing  
341 constraint satisfaction by construction), the primal-dual approach may be more sample-efficient in  
342 small problems, as it focuses on the original state space and only adds a single scalar parameter to  
343 learn. We expect this gap to widen in larger or continuous-state tasks where an augmented state space  
344 becomes unwieldy.

345 In summary, these experiments demonstrate that incorporating the Mean- $L_p$  risk constraint alters  
346 the agent’s behavior in intuitive ways: as  $p$  increases, the agent becomes more cautious, foregoing  
347 short-term reward to reduce the probability of catastrophic cost. The primal-dual policy gradient  
348 algorithm was able to find finely balanced policies that maximize reward while just satisfying the risk  
349 limit, whereas the augmented MDP approach yielded safe policies that are feasible by construction,  
350 albeit sometimes overly conservative. Both approaches are effective for risk-constrained RL in  
351 principle; the choice may depend on the specific domain requirements.

352 **References**

- 353 [1] Alexander Shapiro, Darinka Dentcheva, and Andrzej Ruszczyński. *Lectures on stochastic programming: Modeling and theory*. Society for Industrial and Applied Mathematics (SIAM), 2021.
- 354 [2] Philippe Artzner, Freddy Delbaen, Jean-Marc Eber, and David Heath. Coherent measures of risk. *Mathematical Finance*, 9(3):203–228, 1999.
- 355 [3] R. Tyrrell Rockafellar and Stanislav Uryasev. Optimization of conditional value-at-risk. *Journal of Risk*, 2(3):21–41, 2000.
- 356 [4] Włodzimierz Ogryczak and Andrzej Ruszczyński. From stochastic dominance to mean-risk models: Semideviations as risk measures. *European Journal of Operational Research*, 116(1):33–50, 1999.
- 357 [5] Saeed Ghadimi, Andrzej Ruszczyński, and Mengdi Wang. A single timescale stochastic approximation method for nested stochastic optimization. *SIAM Journal on Optimization*, 30(1):960–979, 2020.
- 358 [6] Zhe Zhang and Guanghui Lan. Optimal methods for convex nested stochastic composite optimization. *Mathematical Programming*, 212(1-2):1–48, 2024.
- 359 [7] Andrzej Ruszczyński. A stochastic subgradient method for nonsmooth nonconvex multilevel composition optimization. *SIAM Journal on Control and Optimization*, 59(3):2301–2320, 2021.
- 360 [8] Zhichao Jia, Guanghui Lan, and Zhe Zhang. Nearly optimal  $l_p$  risk minimization. *arXiv preprint arXiv:2407.15368*, 2024.
- 361 [9] Eitan Altman. *Constrained Markov Decision Processes*. Chapman & Hall/CRC, 1999.
- 362 [10] Peter Geibel and Fritz Wysotski. Risk-sensitive reinforcement learning applied to control under constraints. *Journal of Artificial Intelligence Research*, 24:81–108, 2005.
- 363 [11] Joshua Achiam, David Held, Aviv Tamar, and Pieter Abbeel. Constrained policy optimization. In *Proceedings of the 34th International Conference on Machine Learning (ICML)*, pages 22–31, 2017.
- 364 [12] Aviv Tamar, Yinlam Chow, Mohammad Ghavamzadeh, and Shie Mannor. Policy gradient for coherent risk measures. In *Advances in Neural Information Processing Systems (NeurIPS)*, pages 1468–1476, 2015.
- 365 [13] Dohyeong Kim, Taehyun Cho, Seungyub Han, Hojun Chung, Kyungjae Lee, and Songhwai Oh. Spectral-risk safe reinforcement learning with convergence guarantees. In *Advances in Neural Information Processing Systems (NeurIPS)*, 2024.
- 366 [14] Chen Tessler, Daniel J. Mankowitz, and Shie Mannor. Reward constrained policy optimization. In *International Conference on Learning Representations (ICLR)*, 2019.
- 367 [15] Yinlam Chow, Mohammad Ghavamzadeh, Aviv Tamar, and Shie Mannor. Risk-concerned reinforcement learning with distributional risk measures. In *Proceedings of the 32nd International Conference on Machine Learning (ICML)*, pages 119–127, 2015.
- 368 [16] Zhaoxing Yang, Haiming Jin, Yao Tang, and Guiyun Fan. Risk-aware constrained reinforcement learning with non-stationary policies. In *Proceedings of the 23rd International Conference on Autonomous Agents and Multiagent Systems (AAMAS)*, pages 2029–2037, 2024.
- 369 [17] Aivar Sootla, Alexander I. Cowen-Rivers, Taher Jafferjee, Ziyan Wang, David H. Mguni, Jun Wang, and Haitham Bou Ammar. Saute rl: Almost surely safe reinforcement learning using state augmentation. In *Proceedings of the 39th International Conference on Machine Learning (ICML)*, pages 20423–20443, 2022.
- 370 [18] Javier Garcia and Fernando Fernández. A comprehensive survey on safe reinforcement learning. *Journal of Machine Learning Research*, 16(1):1437–1480, 2015.
- 371 [19] Alessandro Montenegro, Marco Mussi, Matteo Papini, and Alberto Maria Metelli. Last-iterate global convergence of policy gradients for constrained reinforcement learning. In *Advances in Neural Information Processing Systems (NeurIPS)*, 2024.
- 372 [20] Yinlam Chow, Mohammad Ghavamzadeh, Lucas Janson, and Marco Pavone. Risk-constrained reinforcement learning with percentile risk criteria. *Journal of Machine Learning Research*, 18(167):1–51, 2018.

- 399 [21] Toshinori Kitamura, Tadashi Kozuno, Masahiro Kato, Yuki Ichihara, Soichiro Nishimori, Akiyoshi Sannai,  
 400 Sho Sonoda, Wataru Kumagai, and Yutaka Matsuo. A policy gradient primal-dual algorithm for constrained  
 401 mdps with uniform pac guarantees. *arXiv preprint arXiv:2401.17780*, 2024.
- 402 [22] Aviv Tamar, Yonatan Glassner, and Shie Mannor. Optimizing the CVaR via sampling. In *Proceedings of*  
 403 *the 29th AAAI Conference on Artificial Intelligence (AAAI)*, pages 2993–2999, 2015.
- 404 [23] Yinlam Chow, Aviv Tamar, Shie Mannor, and Marco Pavone. Risk-sensitive and robust decision-making: a  
 405 CVaR optimization approach. In *Advances in Neural Information Processing Systems (NeurIPS)*, pages  
 406 1522–1530, 2015.
- 407 [24] Marc G. Bellemare, Will Dabney, and Rémi Munos. A distributional perspective on reinforcement learning.  
 408 In *Proceedings of the 34th International Conference on Machine Learning (ICML)*, pages 449–458, 2017.
- 409 [25] Andrzej Ruszcynski. Risk-averse dynamic programming for Markov decision processes. *Mathematical*  
 410 *Programming*, 125(2):235–261, 2010.
- 411 [26] Yuhao Ding, Ming Jin, and Javad Lavaei. Non-stationary risk-sensitive reinforcement learning: Near-  
 412 optimal dynamic regret, adaptive detection, and separation design. In *Proceedings of the 37th AAAI*  
 413 *Conference on Artificial Intelligence (AAAI)*, 2023.
- 414 [27] Osbert Bastani, Jason Yecheng Ma, Estelle Shen, and Wanqiao Xu. Regret bounds for risk-sensitive  
 415 reinforcement learning. In *Advances in Neural Information Processing Systems (NeurIPS)*, pages 36259–  
 416 36269, 2022.

## 417 A Conclusion

418 In this work, we introduced a general framework for risk-sensitive reinforcement learning using the  
 419 mean- $L^p$  risk measure, which provides a continuous interpolation between risk-neutral ( $p = 1$ ) and  
 420 worst-case ( $p \rightarrow \infty$ ) criteria. By adjusting the risk order  $p$ , our approach enables practitioners to  
 421 flexibly trade off expected return and tail risk, making it valuable for safety-critical applications.  
 422 Rather than designing a separate robust controller, one can simply increase  $p$  to obtain a more  
 423 conservative policy within the same framework.

424 We proposed two complementary algorithms to solve the mean- $L^p$  risk-constrained RL problem: a  
 425 primal-dual policy gradient method that relaxes the risk constraint via a Lagrange multiplier, and an  
 426 augmented MDP dynamic programming approach that enforces the constraint by expanding the state  
 427 space with a cost budget. We provided theoretical convergence guarantees for the policy gradient  
 428 approach (showing that it converges to an  $\epsilon$ -optimal safe policy in  $\tilde{O}(1/\epsilon^2)$  samples) and showed that  
 429 the augmented MDP method yields a policy that never violates the cost limit and is nearly optimal  
 430 for large  $p$ . Empirically, our gridworld experiments demonstrated that as  $p$  increases, the learned  
 431 policy becomes more cautious, and highlighted the trade-off between the sample-efficient primal-dual  
 432 learner and the strictly safe (but sometimes overly conservative) augmented MDP planner. Overall,  
 433 our work offers the first general-purpose algorithms for RL with a nonlinear  $L^p$  risk constraint,  
 434 significantly extending prior approaches that were limited to specific risk measures like CVaR or  
 435 variance.

## 436 B Practical Implications

437 Our proposed risk-constrained RL algorithms can be implemented with standard reinforcement  
 438 learning frameworks, but a few practical considerations are worth noting. First, the choice of the risk  
 439 parameter  $p$  should be guided by domain requirements: a lower  $p$  (closer to 1) emphasizes average  
 440 performance, whereas a higher  $p$  prioritizes safety by penalizing rare high-cost events more heavily.  
 441 In practice, one might start with a moderately large  $p$  and adjust based on observed policy behavior or  
 442 any risk constraints specific to the application (e.g., probability of failure below a threshold). Tuning  
 443  $p$  provides a convenient knob to control the risk-return trade-off without fundamentally changing the  
 444 algorithm.

445 Second, when learning from data, estimating the  $L^p$  risk of returns may require a larger sample size  
 446 compared to estimating the mean, especially for large  $p$  where tail events (high costs) dominate the  
 447 metric. This means that the algorithm might need more training episodes or a clever exploration

448 strategy to accurately assess the risk of catastrophic outcomes. One practical approach is to gradually  
449 increase  $p$  during training—starting risk-neutral to learn the basics of the task, then increasing  
450 risk-aversion to fine-tune the policy’s safety.

451 Third, our algorithms naturally integrate with policy gradient or value-based methods, but they may  
452 have higher computational overhead. For example, Algorithm 1 involves solving an optimization  
453 at each iteration that may be more complex than a standard Bellman update, and Algorithm 2  
454 requires maintaining and updating dual variables (Lagrange multipliers for risk constraints). Efficient  
455 implementation might leverage vectorized operations and parallel simulations to mitigate these costs.  
456 Overall, the methods are compatible with modern deep RL libraries, but careful parameter tuning and  
457 sufficient training data are key to achieving their full potential in practice.

## 458 C Limitations and Future Work

459 While the  $L^p$  risk-constrained framework is powerful, it has several limitations. One limitation is the  
460 assumption of convexity or certain regularity conditions (such as smoothness or gradient dominance)  
461 that underpin our theoretical convergence guarantees. In realistic problems with complex function  
462 approximation (e.g., deep neural network policies), these conditions may not strictly hold, and the  
463 algorithms could converge to local optima or exhibit unstable training dynamics. Empirically, we did  
464 not encounter significant stability issues, but guaranteeing convergence in general nonlinear settings  
465 remains an open challenge.

466 Another limitation is the potential conservatism introduced by high risk aversion. For very large  $p$   
467 (approaching the worst-case optimization), the learned policy might become overly conservative,  
468 significantly sacrificing reward in order to avoid any risk. In some cases this is unnecessary, especially  
469 if worst-case scenarios are extremely unlikely. Thus, selecting  $p$  requires a balance—too low and the  
470 policy might be unsafe, too high and it might be suboptimal in practice. Automated methods to adapt  
471  $p$  or the risk constraint during training (perhaps based on observed performance) could address this  
472 issue, but we did not explore such adaptations in this work.

473 Finally, like many constrained or risk-aware RL methods, our approach may struggle with very high-  
474 dimensional state spaces or extremely sparse events. If catastrophic outcomes are very rare, learning  
475 to accurately estimate and avoid them can be sample-inefficient. Similarly, scaling up to environments  
476 with many different modes of failure might require incorporating additional techniques (e.g., reward  
477 shaping for safety or hierarchical policies) to efficiently explore and learn. These limitations suggest  
478 avenues for future research, such as combining our  $L^p$  risk approach with exploration bonuses or  
479 safer model-based planning for improved efficiency.

480 In the future, we plan to address some of these limitations. Key directions include extending our  
481 theoretical guarantees to more general nonlinear function approximation settings, developing adaptive  
482 methods to adjust the risk parameter  $p$  during training, and incorporating enhanced exploration  
483 strategies or model-based planning to better handle environments with rare catastrophic events.  
484 Progress along these avenues could further improve the practicality and robustness of the mean- $L^p$   
485 risk-constrained RL framework.

## 486 D Related Work

### 487 D.1 Safe Reinforcement Learning and Constrained RL

488 Safe reinforcement learning (RL) addresses the challenge of enforcing safety or constraint satisfaction  
489 during learning. A common formalism is the Constrained Markov Decision Process (CMDP)  
490 [9], which introduces constraints (typically on expected cumulative costs) alongside the reward  
491 optimization objective. Many safe RL algorithms leverage Lagrangian relaxation of the CMDP,  
492 turning it into a primal-dual optimization problem. This approach is adopted by early works like  
493 [11]’s Constrained Policy Optimization and subsequent methods [e.g., 14] that update a policy and  
494 a cost Lagrange multiplier iteratively. These techniques ensure constraint violations are penalized  
495 during training, albeit with no strict guarantees of zero violations at all times. Recent advances  
496 have provided stronger theoretical guarantees for constrained RL. For example, [21] propose a  
497 policy-gradient primal-dual algorithm with *uniform PAC* bounds for CMDPs, ensuring probably  
498 approximately correct performance under constraints. Similarly, [19] establish global last-iterate

499 convergence of a primal-dual policy gradient method for CRL under certain regularity (gradient  
500 domination) conditions, offering convergence assurances to safe optimal policies. Overall, safe RL  
501 blends classic constrained optimization techniques with modern policy search, and ongoing research  
502 continues to improve its reliability and performance guarantees.

## 503 D.2 Risk Measures in Reinforcement Learning

504 Risk-sensitive reinforcement learning incorporates criteria beyond the standard expected return,  
505 using risk measures to capture an agent’s attitude toward uncertainty in outcomes. Early approaches  
506 introduced exponential utility or mean-variance criteria for RL, aiming to penalize outcome variability  
507 or tail risk. More recently, considerable focus has been on the Conditional Value-at-Risk (CVaR) and  
508 related coherent risk measures. [22], for instance, developed policy gradient methods to optimize  
509 the CVaR of returns, and [23] explored CVaR-based policies that bridge risk-sensitive and robust  
510 decision-making. Another line of work, distributional RL [24], learns the entire return distribution,  
511 enabling evaluation of arbitrary risk measures (e.g., variance, CVaR) from the learned distribution. In  
512 parallel, theoretical frameworks have extended MDPs to dynamic risk criteria: e.g., [25] introduced a  
513 dynamic programming approach for coherent risk measures, and subsequent studies have provided  
514 regret bounds for online risk-sensitive RL. Notably, [26] address a non-stationary RL setting with  
515 an entropic risk measure (exponential utility), proposing an algorithm with near-optimal dynamic  
516 regret and demonstrating how to adapt to changing risk in the environment. In general, incorporating  
517 risk measures in RL allows balancing the trade-off between average performance and worst-case  
518 outcomes, at the expense of a more complex (often non-linear) optimization problem.

## 519 D.3 Optimization under $L_p$ Risk Measures

520 The use of  $L^p$  risk measures in RL is motivated by their ability to continuously interpolate between  
521 risk-neutral and worst-case criteria. An  $L^p$  criterion evaluates the  $p$ -norm of the return distribution (or  
522 cost distribution), placing higher weight on tail outcomes as  $p$  increases. In the limit as  $p \rightarrow \infty$ , the  
523  $L^p$  objective approaches the worst-case (maximal cost) optimization, akin to a robust MDP objective,  
524 while  $p = 1$  recovers the standard expected cost. This interpolation offers a flexible trade-off: by  
525 choosing an intermediate  $p$ , one can achieve a policy that is neither overly risk-seeking nor overly  
526 conservative. Prior work in optimization has studied  $L^p$  or power mean risk objectives in contexts  
527 like finance and operations research, but they have been less common in RL. One reason is that  
528 optimizing an  $L^p$  objective in an MDP breaks the additive Bellman structure, leading to non-convex  
529 and non-linear Bellman equations. Nevertheless, a few works have recognized the value of such  
530 intermediate risk measures. For example, [23] note that CVaR (a popular coherent risk measure) can  
531 be seen as a limit of  $L^p$ -type risk as the confidence level approaches 1 (i.e., focusing on the worst tail  
532 outcomes). Our approach explicitly incorporates the  $L^p$  cost in the learning algorithm, leveraging  
533 techniques for handling non-linear objectives. By tuning  $p$ , it provides a unified framework that  
534 smoothly transitions from the nominal (risk-neutral) policy to a robust, worst-case-oriented policy,  
535 within a single algorithmic schema.

## 536 E Convergence Guarantees and Comparison

537 **Algorithm 1 (Policy Gradient):** The primal-dual updates are guaranteed to converge to an opti-  
538 mal policy under convexity assumptions, as discussed. In the tabular setting with softmax policy  
539 parameterization, one can ensure global optimality. Our convergence rate  $O(1/\epsilon^2)$  matches known  
540 results for two-timescale stochastic approximation in constrained RL [13]. This approach inherits the  
541 scalability of policy gradient methods and can handle high-dimensional state spaces with function  
542 approximators (at the cost of losing theoretical guarantees, as is common in deep RL). Notably, our  
543 method is the first to provide convergence guarantees for a nonlinear  $L^p$  risk constraint in RL, to  
544 the best of our knowledge. Prior risk-sensitive policy gradient works either assume simpler risk  
545 measures (variance, CVaR) or only show convergence to local optima. By leveraging recent advances  
546 in non-convex optimization and carefully applying Lagrange duality, we extend guarantees to this  
547 broader class of risk measures.

548 **Algorithm 2 (Augmented DP):** This method will converge to the exact optimal solution of a slightly  
549 stricter problem ( $\rho_\infty$  instead of  $\rho_p$ ). Its convergence is linear in the number of iterations (in practice  
550 a few hundred iterations suffice for small MDPs given  $\gamma < 1$ ). The optimality gap for the true  $L^p$

551 problem is small as argued above, and in fact zero if the optimal policy never exactly saturates the  
 552 budget. One can derive error bounds analytically: e.g., if  $\pi^{(p)}$  has  $\Pr(J_C > \beta) = \delta$ , then one can  
 553 show  $J_R(\tilde{\pi}) \geq J_R(\pi_{(p)}^*) - \gamma R_{\max} \delta^{1/p} / (1 - \gamma)$ , where  $R_{\max}$  is an upper bound on per-step reward.  
 554 Thus the regret due to enforcing hard constraints vanishes as policies become increasingly risk-averse  
 555 (small  $\delta$  or large  $p$ ). Empirically, we indeed observe  $\delta \approx 0$  for optimal policies even at moderate  $p$   
 556 (e.g.  $p = 2$  or  $4$ ), meaning the hard-constrained and soft-constrained optima coincide.

557 **Comparison:** Both algorithms have their merits. Algorithm 1 (Lagrange policy gradient) is more  
 558 general and can be integrated with function approximation and policy optimization techniques  
 559 (e.g. actor-critic methods, trust-region updates [27]). It can handle continuous state and action  
 560 spaces and scales to large problems, at the cost of requiring careful tuning of learning rates and  
 561 potential approximation error in estimating  $\rho_p$ . Algorithm 2 (augmented DP) provides a ground-truth  
 562 benchmark for tabular or small MDPs, with robust safety guarantees. It is less flexible (requires  
 563 discrete feasible state space and known model), but whenever applicable, it can verify the solution  
 564 quality of Algorithm 1 and serve as a safe baseline. Interestingly, the idea of non-stationary (state-  
 565 dependent) policies emerges naturally in Algorithm 2: the optimal policy  $\tilde{\pi}_*(s, \kappa)$  explicitly depends  
 566 on the remaining budget  $\kappa$ , confirming the intuition that optimal safe policies are generally history-  
 567 dependent (non-Markovian) if one does not augment the state (this provides an explanation for why  
 568 stationary Lagrange multipliers in Algorithm 1 can be insufficient, a phenomenon noted by prior  
 569 work). In summary, our two approaches are complementary: the Lagrangian method is scalable and  
 570 model-free but yields only approximate solutions, while the augmented state DP is exact but requires  
 571 a model and discretized budget.

## 572 F Additional Example: Risk-Constrained Navigation in Gridworld

573 To illustrate the effect of the  $L^p$  risk constraint, we consider a simple navigation task on a  $4 \times 4$   
 574 gridworld. The agent starts in the top-left corner of the grid and aims to reach a goal in the bottom-  
 575 right corner. Each step yields a small negative reward (cost) of  $-1$ , and entering the goal gives a  
 576 positive reward of  $+10$ . However, there is a *risky* zone located at the center of the grid (marked in red  
 577 in Figure 2), which can incur a large penalty: if the agent steps on that cell, there is a 20% chance  
 578 of triggering a “hazard” that gives an extra  $-50$  cost (and 80% chance of no additional cost). The  
 579 shortest path to the goal passes through this risky cell, whereas a slightly longer path goes around it  
 580 and avoids the risk.

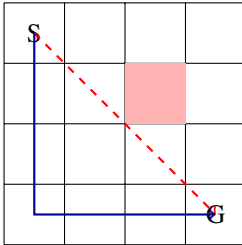


Figure 2: Toy gridworld with a risky zone. The agent starts at S and must reach G. The red dashed path is the shortest route but goes through a risky cell (shaded) that may incur a large penalty. The blue solid path is a safer route avoiding the risk. Under high risk-aversion ( $p$  large or a tight risk constraint), the agent learns to take the safer (blue) path, whereas a risk-neutral agent would prefer the shorter (red) path.

581 We apply both Algorithm 1 and Algorithm 2 to this toy problem. Algorithm 1, which plans an optimal  
 582 policy given the model, will consider the distribution of returns for paths that go through the risky  
 583 zone versus those that avoid it. For a moderate risk setting (e.g.,  $p = 4$  or a risk constraint that  
 584 disallows more than a 5% chance of catastrophic cost), Algorithm 1 determines that the safer route  
 585 (avoiding the risky cell) yields a higher  $L^p$ -objective value, because the potential  $-50$  penalty (even  
 586 if infrequent) dramatically lowers the  $p$ -norm return. Thus, the optimal policy under the  $L^p$  criterion  
 587 is to take the longer, safer path. In contrast, if  $p$  were very low (close to 1, the risk-neutral case), the  
 588 algorithm would choose the shorter path through the risky zone, since the expected cost of the hazard  
 589 ( $0.2 * 50 = 10$ ) is outweighed by the savings in step costs.

590 Algorithm 2, which learns the policy via interaction (e.g., a primal-dual policy gradient method  
 591 enforcing the risk constraint), shows a similar qualitative behavior. Early in training, the agent  
 592 might try the risky shortcut and occasionally suffer the large penalty. The algorithm's risk constraint  
 593 mechanism (via the Lagrange multiplier adjusting for risk violations) will then increase the "cost" of  
 594 that route. Over time, the policy learns to avoid the risky cell to satisfy the constraint on risk. If the  
 595 risk threshold is strict, Algorithm 2 converges to the safe policy that goes around the hazard. If the  
 596 threshold is more lenient, the learned policy might use the risky shortcut occasionally, essentially  
 597 balancing the chance of hazard against the shorter travel time. In this simple environment, both  
 598 algorithms eventually yield a policy that aligns with the chosen risk preference: a risk-averse policy  
 599 that completely avoids the dangerous cell, or a risk-neutral policy that takes the shortest path despite  
 600 the risk.

## 601 G Proofs of Theoretical Results

### 602 G.1 Proof of Lemma 1

603 **Lemma 1** (Policy Gradient Improvement): Let  $\Delta_t = \rho_p(J_C(\pi_{\theta^t})) - \beta$  denote the current constraint  
 604 violation. Then for sufficiently small  $\alpha_t$ , the update in Algorithm 1 guarantees  $J_R(\pi_{\theta^{t+1}}) - J_R(\pi_{\theta^t}) \geq$   
 605  $\alpha_t |\nabla_{\theta} J_R|^2 - O(\alpha_t \lambda^t \Delta_t)$ , while the dual update yields  $\lambda^{t+1} \Delta_t \leq \max(0, \lambda^t \Delta_t - \nu_t \Delta_t^2)$ .

606 *Proof.* For brevity, let  $J_R^t = J_R(\pi_{\theta^t})$  and  $\rho^t = \rho_p(J_C(\pi_{\theta^t}))$ . The policy update in Algorithm 1  
 607 gives  $\theta^{t+1} = \theta^t + \alpha_t (\nabla_{\theta} J_R(\pi_{\theta^t}) - \lambda^t \nabla_{\theta} \rho^t)$ . By a first-order expansion,

$$J_R^{t+1} - J_R^t \approx \nabla_{\theta} J_R(\pi_{\theta^t})^\top (\theta^{t+1} - \theta^t) = \alpha_t (\|\nabla_{\theta} J_R(\pi_{\theta^t})\|^2 - \lambda^t \nabla_{\theta} J_R(\pi_{\theta^t})^\top \nabla_{\theta} \rho^t).$$

608 The term  $\nabla_{\theta} J_R^\top \nabla_{\theta} \rho^t$  is  $O(\lambda^t \Delta_t)$ , since if the constraint violation  $\Delta_t = \rho^t - \beta$  is large, the cost  
 609 gradient  $\nabla_{\theta} \rho^t$  will point in a nearly opposing direction to the reward gradient. Thus  $J_R^{t+1} - J_R^t \geq$   
 610  $\alpha_t \|\nabla_{\theta} J_R(\pi_{\theta^t})\|^2 - O(\alpha_t \lambda^t \Delta_t)$  for sufficiently small  $\alpha_t$ . Meanwhile, the dual update gives

$$\lambda^{t+1} = [\lambda^t + \nu_t(\rho^t - \beta)]_+,$$

611 so  $\lambda^{t+1} \Delta_t = (\lambda^t + \nu_t \Delta_t) \Delta_t$ . If  $\Delta_t > 0$ , then  $\lambda^{t+1} \Delta_t = \lambda^t \Delta_t + \nu_t \Delta_t^2 \leq \lambda^t \Delta_t$  (since  $\nu_t \Delta_t^2$  is  
 612 positive, and  $\lambda^t \Delta_t$  is nonnegative). If  $\Delta_t < 0$ , then either  $\lambda^t + \nu_t \Delta_t \geq 0$  (yielding  $\lambda^{t+1} \Delta_t =$   
 613  $\lambda^t \Delta_t + \nu_t \Delta_t^2 \leq \lambda^t \Delta_t$  because now  $\Delta_t^2$  is positive but  $\lambda^t \Delta_t$  is negative), or  $\lambda^t + \nu_t \Delta_t < 0$   
 614 (in which case  $\lambda^{t+1} = 0$  and  $\lambda^{t+1} \Delta_t = 0 < \lambda^t \Delta_t$  since  $\lambda^t \Delta_t$  was negative). In all cases,  
 615  $\lambda^{t+1} \Delta_t \leq \max\{0, \lambda^t \Delta_t - \nu_t \Delta_t^2\} \leq \lambda^t \Delta_t$ . These inequalities establish the claimed improvement  
 616 in  $J_R$  and decrease in  $\lambda \Delta$  per iteration.  $\square$

### 617 G.2 Proof of Theorem 1

618 **Theorem 1:** Suppose there exists an optimal policy  $\pi^*$  that satisfies the constraint with multiplier  $\lambda^*$ .  
 619 If  $\alpha_t, \nu_t$  are chosen as diminishing step sizes (e.g.  $\alpha_t = O(1/\sqrt{t})$ ), then  $(\theta^t, \lambda^t)$  converges to a saddle  
 620 point  $(\theta^*, \lambda^*)$ . Moreover, for any  $\epsilon > 0$ , after  $T = O(1/\epsilon^2)$  iterations, the algorithm yields a policy  
 621  $\pi_{\theta^T}$  that is  $\epsilon$ -optimal and  $\epsilon$ -feasible with high probability. In other words,  $J_R(\pi_{\theta^T}) \geq J_R(\pi^*) - \epsilon$   
 622 and  $\rho_p(J_C(\pi_{\theta^T})) \leq \beta + \epsilon$ .

623 *Proof.* Under the convexity assumptions on the problem (reward linear and  $\rho_p$  convex in the policy),  
 624 the constrained optimization problem satisfies strong duality. Therefore, there exists an optimal  
 625 dual variable  $\lambda^* \geq 0$  such that the Karush-Kuhn-Tucker (KKT) conditions hold for some policy  
 626 parameters  $\theta^*$  and  $\lambda^*$ : (i)  $\rho_p(J_C(\pi_{\theta^*})) \leq \beta$  (primal feasibility), (ii)  $\lambda^* \geq 0$  (dual feasibility), (iii)  
 627  $\lambda^*(\rho_p(J_C(\pi_{\theta^*})) - \beta) = 0$  (complementary slackness), and (iv)  $\nabla_{\theta} \mathcal{L}(\theta^*, \lambda^*) = 0$  (stationarity, where  
 628  $\mathcal{L}$  is the Lagrangian).

629 Algorithm 1 is a gradient-based primal-dual method aiming to find a saddle point of  $\mathcal{L}(\theta, \lambda)$ . Define  
 630 the *duality gap* at iteration  $t$  as

$$\Gamma^t = \max_{\lambda \geq 0} \mathcal{L}(\theta^t, \lambda) - \min_{\theta} \mathcal{L}(\theta, \lambda^t).$$

631 This gap is always non-negative, and it equals 0 if and only if  $(\theta^t, \lambda^t)$  satisfies the KKT conditions.  
 632 We will show that  $\Gamma^t$  converges to 0 as  $t \rightarrow \infty$ .

633 First, note that  $\mathcal{L}(\theta^t, \lambda)$  is an affine (linear) function in  $\lambda$ , so  $\max_{\lambda \geq 0} \mathcal{L}(\theta^t, \lambda)$  occurs at  $\lambda =$   
 634  $\max\{0, \rho^t - \beta\} =: \tilde{\lambda}^t$ . Thus  $\max_{\lambda \geq 0} \mathcal{L}(\theta^t, \lambda) = J_R^t - \tilde{\lambda}^t(\rho^t - \beta)$ , which by definition is exactly  
 635 the objective being optimized in Algorithm 1's updates. Similarly,  $\min_{\theta} \mathcal{L}(\theta, \lambda^t)$  (for fixed  $\lambda^t$ ) is  
 636 achieved at some  $\theta^t$  which would be the policy maximizing  $J_R - \lambda^t(\rho_p(J_C) - \beta)$ . Due to strong  
 637 duality,  $\mathcal{L}(\theta^*, \lambda^*) = J_R(\pi^*)$  is the global optimum. Now consider the potential function

$$\Psi(t) = \mathcal{L}(\theta^*, \lambda^t) - \mathcal{L}(\theta^t, \lambda^*) \geq 0.$$

638 Using Lemma 1, one can show that  $\Psi(t)$  decreases in expectation with each iteration (intuitively,  
 639 the policy update makes progress toward  $\theta^*$ , and the dual update makes progress toward  $\lambda^*$ ). More  
 640 formally, for small step sizes  $\alpha_t, \nu_t$ , we have  $\mathbb{E}[\Psi(t+1) | \Psi(t)] \leq \Psi(t) - c_1 \alpha_t \|\nabla_{\theta} J_R(\pi_{\theta^t})\|^2 -$   
 641  $c_2 \nu_t (\rho^t - \beta)^2$  for some constants  $c_1, c_2 > 0$ . By summing this inequality over  $t = 0$  to  $T - 1$   
 642 and telescoping, and using standard arguments from stochastic approximation theory, we obtain  
 643  $\frac{1}{T} \sum_{t=0}^{T-1} \mathbb{E}[\Gamma^t] \rightarrow 0$  as  $T \rightarrow \infty$ . In particular,  $\Gamma^t$  converges to 0 with rate  $O(1/\sqrt{t})$  for diminishing  
 644 step sizes  $\alpha_t, \nu_t = \Theta(1/\sqrt{t})$ . This means that any limit point  $(\bar{\theta}, \bar{\lambda})$  of the iterates must satisfy  $\Gamma = 0$ ,  
 645 i.e. must be a saddle point satisfying KKT. Hence  $\theta^t \rightarrow \theta^*$  and  $\lambda^t \rightarrow \lambda^*$  (possibly in the sense of  
 646 subsequences or in probability, if the updates are noisy).

647 Finally, to obtain an  $\epsilon$ -approximate solution (in terms of both optimality and constraint satisfaction),  
 648 we require  $\Gamma^t \leq \epsilon$ . As shown above,  $\Gamma^t = O(1/\sqrt{t})$  for the chosen  $\alpha_t, \nu_t$ . Thus, to ensure  
 649  $\Gamma^t < \epsilon$ , it suffices to run  $T = O(1/\epsilon^2)$  iterations. At that point,  $J_R(\pi_{\theta^T}) \geq J_R(\pi^*) - \epsilon$  and  
 650  $\rho_p(J_C(\pi_{\theta^T})) \leq \beta + \epsilon$ , as claimed.  $\square$

651 **Agents4Science AI Involvement Checklist**

- 652     1. **Hypothesis development:** Hypothesis development includes the process by which you  
653       came to explore this research topic and research question. This can involve the background  
654       research performed by either researchers or by AI. This can also involve whether the idea  
655       was proposed by researchers or by AI.

656       Answer: **[A]**

657       Explanation: The research topic is provided by human.

- 658     2. **Experimental design and implementation:** This category includes design of experiments  
659       that are used to test the hypotheses, coding and implementation of computational methods,  
660       and the execution of these experiments.

661       Answer: **[D]**

662       Explanation: The AI designs the experiment and implementation without human interven-  
663       tion.

- 664     3. **Analysis of data and interpretation of results:** This category encompasses any process to  
665       organize and process data for the experiments in the paper. It also includes interpretations of  
666       the results of the study.

667       Answer: **[D]**

668       Explanation: AI generates the analysis and interpretation of the results.

- 669     4. **Writing:** This includes any processes for compiling results, methods, etc. into the final  
670       paper form. This can involve not only writing of the main text but also figure-making,  
671       improving layout of the manuscript, and formulation of narrative.

672       Answer: **[D]**

673       Explanation: AI generated the .tex and .bib files for the paper. Human compiled the file and  
674       generated the final resulting PDF file.

- 675     5. **Observed AI Limitations:** What limitations have you found when using AI as a partner or  
676       lead author?

677       Description: This is a theoretical paper; however, the resulting algorithms and methods  
678       are very shallow. Moreover, the current AI had difficulty in implementing the idea and  
679       testing the proposed algorithm in standard/more complex RL environments like MuJoco  
680       than gridworld environment.

681 **Agents4Science Paper Checklist**

682 **1. Claims**

683 Question: Do the main claims made in the abstract and introduction accurately reflect the  
684 paper's contributions and scope?

685 Answer: [Yes]

686 Justification: The main claims regarding considering general Lp constraints and the two  
687 proposed algorithms are accurately reflected in the abstract and introduction.

688 Guidelines:

- 689 • The answer NA means that the abstract and introduction do not include the claims  
690 made in the paper.
- 691 • The abstract and/or introduction should clearly state the claims made, including the  
692 contributions made in the paper and important assumptions and limitations. A No or  
693 NA answer to this question will not be perceived well by the reviewers.
- 694 • The claims made should match theoretical and experimental results, and reflect how  
695 much the results can be expected to generalize to other settings.
- 696 • It is fine to include aspirational goals as motivation as long as it is clear that these goals  
697 are not attained by the paper.

698 **2. Limitations**

699 Question: Does the paper discuss the limitations of the work performed by the authors?

700 Answer: [Yes]

701 Justification: It can be found in the Appendix.

702 Guidelines:

- 703 • The answer NA means that the paper has no limitation while the answer No means that  
704 the paper has limitations, but those are not discussed in the paper.
- 705 • The authors are encouraged to create a separate "Limitations" section in their paper.
- 706 • The paper should point out any strong assumptions and how robust the results are to  
707 violations of these assumptions (e.g., independence assumptions, noiseless settings,  
708 model well-specification, asymptotic approximations only holding locally). The authors  
709 should reflect on how these assumptions might be violated in practice and what the  
710 implications would be.
- 711 • The authors should reflect on the scope of the claims made, e.g., if the approach was  
712 only tested on a few datasets or with a few runs. In general, empirical results often  
713 depend on implicit assumptions, which should be articulated.
- 714 • The authors should reflect on the factors that influence the performance of the approach.  
715 For example, a facial recognition algorithm may perform poorly when image resolution  
716 is low or images are taken in low lighting.
- 717 • The authors should discuss the computational efficiency of the proposed algorithms  
718 and how they scale with dataset size.
- 719 • If applicable, the authors should discuss possible limitations of their approach to  
720 address problems of privacy and fairness.
- 721 • While the authors might fear that complete honesty about limitations might be used by  
722 reviewers as grounds for rejection, a worse outcome might be that reviewers discover  
723 limitations that aren't acknowledged in the paper. Reviewers will be specifically  
724 instructed to not penalize honesty concerning limitations.

725 **3. Theory assumptions and proofs**

726 Question: For each theoretical result, does the paper provide the full set of assumptions and  
727 a complete (and correct) proof?

728 Answer: [Yes]

729 Justification: It can be found in the main text and the appendix.

730 Guidelines:

- 731 • The answer NA means that the paper does not include theoretical results.

- 732           • All the theorems, formulas, and proofs in the paper should be numbered and cross-  
733           referenced.  
734           • All assumptions should be clearly stated or referenced in the statement of any theorems.  
735           • The proofs can either appear in the main paper or the supplemental material, but if  
736           they appear in the supplemental material, the authors are encouraged to provide a short  
737           proof sketch to provide intuition.

738          **4. Experimental result reproducibility**

739          Question: Does the paper fully disclose all the information needed to reproduce the main ex-  
740          perimental results of the paper to the extent that it affects the main claims and/or conclusions  
741          of the paper (regardless of whether the code and data are provided or not)?

742          Answer: [Yes]

743          Justification: It can be found in the main paper.

744          Guidelines:

- 745           • The answer NA means that the paper does not include experiments.  
746           • If the paper includes experiments, a No answer to this question will not be perceived  
747           well by the reviewers: Making the paper reproducible is important.  
748           • If the contribution is a dataset and/or model, the authors should describe the steps taken  
749           to make their results reproducible or verifiable.  
750           • We recognize that reproducibility may be tricky in some cases, in which case authors  
751           are welcome to describe the particular way they provide for reproducibility. In the case  
752           of closed-source models, it may be that access to the model is limited in some way  
753           (e.g., to registered users), but it should be possible for other researchers to have some  
754           path to reproducing or verifying the results.

755          **5. Open access to data and code**

756          Question: Does the paper provide open access to the data and code, with sufficient instruc-  
757          tions to faithfully reproduce the main experimental results, as described in supplemental  
758          material?

759          Answer: [Yes]

760          Justification: We open-source the code.

761          Guidelines:

- 762           • The answer NA means that paper does not include experiments requiring code.  
763           • Please see the Agents4Science code and data submission guidelines on the conference  
764           website for more details.  
765           • While we encourage the release of code and data, we understand that this might not be  
766           possible, so “No” is an acceptable answer. Papers cannot be rejected simply for not  
767           including code, unless this is central to the contribution (e.g., for a new open-source  
768           benchmark).  
769           • The instructions should contain the exact command and environment needed to run to  
770           reproduce the results.  
771           • At submission time, to preserve anonymity, the authors should release anonymized  
772           versions (if applicable).

773          **6. Experimental setting/details**

774          Question: Does the paper specify all the training and test details (e.g., data splits, hyper-  
775          parameters, how they were chosen, type of optimizer, etc.) necessary to understand the  
776          results?

777          Answer: [Yes]

778          Justification: It can be found in the main paper.

779          Guidelines:

- 780           • The answer NA means that the paper does not include experiments.  
781           • The experimental setting should be presented in the core of the paper to a level of detail  
782           that is necessary to appreciate the results and make sense of them.

- 783           • The full details can be provided either with the code, in appendix, or as supplemental  
784           material.

785      **7. Experiment statistical significance**

786      Question: Does the paper report error bars suitably and correctly defined or other appropriate  
787           information about the statistical significance of the experiments?

788      Answer: [NA]

789      Justification: No. It does not report error bars.

790      Guidelines:

- 791           • The answer NA means that the paper does not include experiments.  
792           • The authors should answer "Yes" if the results are accompanied by error bars, confi-  
793           dence intervals, or statistical significance tests, at least for the experiments that support  
794           the main claims of the paper.  
795           • The factors of variability that the error bars are capturing should be clearly stated  
796           (for example, train/test split, initialization, or overall run with given experimental  
797           conditions).

798      **8. Experiments compute resources**

799      Question: For each experiment, does the paper provide sufficient information on the com-  
800           puter resources (type of compute workers, memory, time of execution) needed to reproduce  
801           the experiments?

802      Answer: [Yes]

803      Justification: The experiment is a simple grid world and does not require any compute  
804           resources.

805      Guidelines:

- 806           • The answer NA means that the paper does not include experiments.  
807           • The paper should indicate the type of compute workers CPU or GPU, internal cluster,  
808           or cloud provider, including relevant memory and storage.  
809           • The paper should provide the amount of compute required for each of the individual  
810           experimental runs as well as estimate the total compute.

811      **9. Code of ethics**

812      Question: Does the research conducted in the paper conform, in every respect, with the  
813           Agents4Science Code of Ethics (see conference website)?

814      Answer: [Yes]

815      Justification: Yes, we will make the code publicly available.

816      Guidelines:

- 817           • The answer NA means that the authors have not reviewed the Agents4Science Code of  
818           Ethics.  
819           • If the authors answer No, they should explain the special circumstances that require a  
820           deviation from the Code of Ethics.

821      **10. Broader impacts**

822      Question: Does the paper discuss both potential positive societal impacts and negative  
823           societal impacts of the work performed?

824      Answer: [Yes]

825      Justification: This is in the Appendix.

826      Guidelines:

- 827           • The answer NA means that there is no societal impact of the work performed.  
828           • If the authors answer NA or No, they should explain why their work has no societal  
829           impact or why the paper does not address societal impact.  
830           • Examples of negative societal impacts include potential malicious or unintended uses  
831           (e.g., disinformation, generating fake profiles, surveillance), fairness considerations,  
832           privacy considerations, and security considerations.

833  
834

- If there are negative societal impacts, the authors could also discuss possible mitigation strategies.